

show the presence of only one Ti—i.e., Ti(III) species (Figure 8) confirming the complete conversion of Ti(IV) to Ti(III). Also, this affirms the statement made earlier that Ti(III) is soluble to some extent in the acidic melt.

Ethylene Polymerization. A logical extension of the Ti chemistry in these melts is to test for catalytic olefin polymerization. To this end, 0.5 g of AlEtCl₂ and 0.5 g of TiCl₄ were combined in 7.2 g of 1.1:1.0 AlCl₃–ImCl, resulting in the immediate production of a deep red solution. Bubbling ethylene into the melt at 1 atm induced the formation of a brown-green cloudiness. After several minutes of ethylene bubbling, the reaction was quenched with MeOH. Flakes of polyethylene were seen floating in the resulting clear MeOH solution. The polyethylene flakes (mp: 120–130 °C) were isolated via centrifugation. Although the yield of polyethylene was too low to quantitate, it is significant that the ambient-temperature molten salt can serve as a medium for catalytic polyethylene production. Higher yields of polyethylene

have been achieved in acidic melts employing the homogeneous catalyst system: Cp₂TiCl₂/alkylaluminums.²⁸

Conclusions

The AlCl₃–ImCl molten salt offers a unique medium for the examination of metal halides. It is an aprotic solvent that allows examination of the electrochemistry and spectroscopic properties of chloro complexes without coordination sphere changes often induced in organic solvents. Also, because it is used at ambient temperatures, it is possible to carry out organometallic reactions, e.g. metal alkylations, in the melts.

Acknowledgment. This work was supported by the Air Force Office of Scientific Research. We thank Dr. Janet Morrow for use of her spectroscopic equipment.

(28) Carlin, R. T.; Wilkes, J. S. To be submitted for publication.

Contribution from the Department of Chemistry,
Wayne State University, Detroit, Michigan 48202

Tetranuclear Complexes of 1,3,5,9,11,13-Hexaketonates. 2. Synthesis and Electrochemistry of a Series of Heterotetranuclear Complexes, Bis{1,1'-(1,3-phenylene)bis[7-methyl-1,3,5-octanetrionato(4-)]}hexakis(pyridine)bis[di-oxouranium(VI)]dimetal(II), M₂(UO₂)₂(MOB)₂(py)₆

R. L. Lintvedt,* W. E. Lynch, and J. K. Zehetmair

Received July 24, 1989

A series of heterotetranuclear complexes was prepared by using a 1,3,5,9,11,13-hexaketonate ligand. The specific ligand used in this study contains two 1,3,5-triketone groups substituted at the meta positions of a benzene ring. Neutral complexes are formed by binding four dicationic metal species to two tetraanionic ligands. The resulting tetranuclear complexes contain two binuclear moieties separated by about 7 Å. A series of complexes with two uranyl ions and two metal ions, M²⁺, per molecule was prepared. Reaction of the ligand with UO₂²⁺ results in the selective coordination of the uranium to the "outside" (1,3 and 11,13) coordination sites of the hexaketonates. As a result, the UO₂²⁺ ions assemble the ligands so that the "interior" (3,5 and 9,11) coordination sites are available for binding the divalent metal ions M²⁺. The electrochemical properties of the resulting M₂(UO₂)₂(L)₂ complexes were investigated by cyclic voltammetry, chronoamperometry, and controlled-potential electrolysis. The nature of the multi-electron-transfer processes observed is discussed on the basis of the results of these experiments.

Introduction

Cooperative interactions between metal ions in polynuclear complexes continue to be a subject of considerable interest. An important part of this subject is the interactions between different metal ions in heteropolynuclear complexes. A difficulty that arises immediately when one attempts to address this problem is systematically designing and synthesizing pure compounds. Initially, we developed a strategy¹ that depends upon (1) using binucleating ligands with two different coordination environments, (2) selectively binding one metal ion to one of the sites and characterizing the mononuclear precursor, and (3) adding to the precursor complex a different metal ion that binds to the second site. This approach obviously is only applicable with unsymmetric ligands that have a significant sites selectivity for the metal ions of interest.

Another synthetic approach has been developed that is applicable to symmetric polynucleating ligands.^{2–4} This involves preparing a mononuclear precursor complex in which the first metal ion assembles the ligands in a manner that facilitates the incorporation of the second, different metal ion. The UO₂²⁺ ion is very well suited to this approach because of its strong tendency to bind a fifth equatorial ligand. The resulting geometry forces a "cis" arrangement of the principal equatorial ligand and positions

them to bind a second metal ion. This is shown in Figure 1 for the mononuclear UO₂²⁺ complex of 1,5-diphenyl-1,3,5-pentane-trionate, UO₂(HDBA)₂(CH₃OH).² This precursor complex was used to prepare a series of heterobinuclear compounds containing a symmetric triketonate ligand.³

The same approach has been used to prepare heterotrimeric complexes of a symmetric *tetraketonate*, 1,7-diphenyl-1,3,5,7-heptanetetraone (H₃DBAA).⁴ In this case, two UO₂²⁺ ions preferentially bind to the terminal coordination sites (1,3 and 5,7) because of the stereochemical requirements of the fifth equatorial ligands. The central position (3,5) is available for binding a transition-metal ion. The structures of four compounds with the general formula M(UO₂)₂(DBAA)₂(py)₄ where M = Ni(II), Co(II), Fe(II), and Mn(II) were determined.⁴ All are isomorphous. The structure is shown in Figure 2.

The electrochemistry of trinuclear M(UO₂)₂(DBAA)₂(py)₄ complexes showed very interesting patterns in which there is obvious communication between the U centers. The strength of the interaction between the uranium centers is sensitive to the identity of the M(II) metal ion and increases in the order Fe < Co < Ni < Cu < Zn. The present study was undertaken to investigate further the nature of the interactions in heteronuclear complexes containing the uranyl ion.

Experimental Section

I. Ligand Synthesis. A 1,3,7,9-tetraketonate, 1,1'-(1,3-phenylene)bis-(4,4-dimethyl-1,3-pentanedione), abbreviated H₂DPB, was prepared by condensing dimethyl isophthalate and 3,3-dimethyl-2-butanone in THF with NaH. The product was recrystallized from methanol. Anal. Calcd for C₂₀H₂₆O₄: C, 72.69; H, 7.31. Found: C, 71.98; H, 7.26. Mp: 100 °C.

- (1) Tomlonovic, B. K.; Hough, R. L.; Glick, M. D.; Lintvedt, R. L. *J. Am. Chem. Soc.* **1975**, *97*, 2925.
- (2) Lintvedt, R. L.; Heeg, M. J.; Ahmad, N.; Glick, M. D. *Inorg. Chem.* **1982**, *21*, 2350.
- (3) Lintvedt, R. L.; Ahmad, N. *Inorg. Chem.* **1982**, *21*, 2356.
- (4) Lintvedt, R. L.; Schoenfelner, B. A.; Ciccarelli, C.; Glick, M. D. *Inorg. Chem.* **1984**, *23*, 2867.

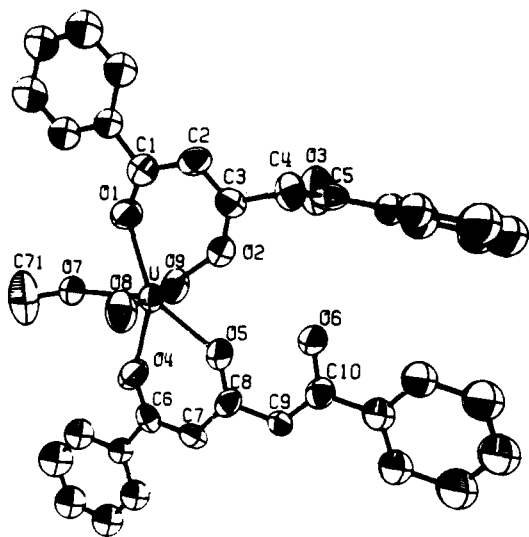


Figure 1. Structure of a triketonate uranyl complex, $\text{UO}_2(\text{HDBA})_2 \cdot (\text{CH}_3\text{OH})$.

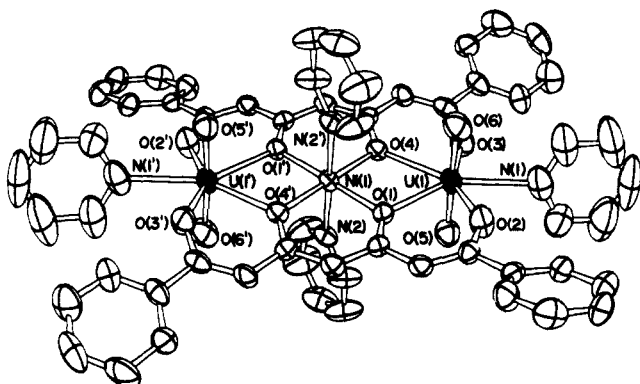


Figure 2. Structure of a tetraketonate uranyl complex, $\text{Ni}(\text{UO}_2)_2(\text{DBAA})_2(\text{py})_4$.

A 1,3,5,9,11,13-hexaketone, 1,1'-(1,3-phenylene)bis(7-methyl-1,3,5-octanetrione), abbreviated H_4MOB , was prepared by condensing dimethyl isophthalate and 6-methyl-2,4-heptanedione. The synthesis and characterization has been reported.⁵

II. Synthesis of Complexes. **Bis[1,1'-(1,3-phenylene)bis[4,4-dimethyl-1,3-pentanedionato(2-)]bis(pyridine)bis(dioxouranium(VI))], $(\text{UO}_2)_2(\text{DPB})_2(\text{py})_2$.** Reagent grade $\text{UO}_2(\text{OAc})_2 \cdot 2\text{H}_2\text{O}$ (2.57 g, 0.0061 mol) was refluxed in 100 mL of methanol. After 10 min a solution of the ligand H_2DPB (0.20 g, 0.0061 mol) and 2 mL of triethylamine in 150 mL of methanol was added. The resulting mixture was refluxed for 24 h and filtered hot. The solid was washed with water and then acetone. Recrystallization from pyridine yields a bright yellow powder that decomposes above 300 °C. Anal. Calcd for $\text{U}_2\text{C}_{50}\text{H}_{58}\text{N}_2\text{O}_{12}$: C, 44.31; H, 4.32; N, 2.07; U, 35.12. Found: C, 44.38; H, 4.31; N, 2.39; U, 33.84.

Bis[1,1'-(1,3-phenylene)bis[7-methyl-1,3,5-octanetrionato(4-)]tetrakis(pyridine)tetrakis(II)-Bis(pyridine)], $\text{Zn}_4(\text{MOB})_2(\text{py})_4 \cdot 2\text{py}$. Reagent grade $\text{Zn}(\text{OAc})_2 \cdot 2\text{H}_2\text{O}$ was dissolved in about 200 mL of refluxing methanol. A solution of H_4MOB (1 g, 0.0026 mol) and triethylamine (1.45 mL, 0.010 mol) in 150 mL of methanol was added to the refluxing solution of $\text{Zn}(\text{OAc})_2 \cdot 2\text{H}_2\text{O}$. The resulting solution was refluxed for 1 h, after which the volume of the solvent was reduced and a yellow solid was collected on a filter. Recrystallization from pyridine yields bright yellow needles that do not melt up to 360 °C. Anal. Calcd for $\text{Zn}_4\text{C}_{73}\text{H}_{77}\text{N}_5\text{O}_{12}$: C, 59.39; H, 5.26; N, 4.74; Zn, 17.69. Found: C, 58.72; H, 5.10; N, 4.57; Zn, 17.24.

Bis[1,1'-(1,3-phenylene)bis[7-methyl-1,3,5-octanetrionato(4-)]hexakis(pyridine)bis(dioxouranium(VI))dimetal(II)], $\text{M}_2(\text{UO}_2)_2(\text{MOB})_2(\text{py})_6$. The ligand H_4MOB (1 g, 0.0026 mol) was refluxed for 15 min in 250 mL of MeOH. This solution was cooled to room temperature, and finely powdered reagent grade $(\text{UO}_2)(\text{OAc})_2 \cdot 2\text{H}_2\text{O}$ (1.15 g, 0.0026 mol) was added. The solution was stirred until it became a translucent red color (10–20 min). At this point reagent grade $\text{M}(\text{OAc})_2 \cdot x\text{H}_2\text{O}$ (0.0026 mol)

Table I. Elemental Analyses for the $\text{M}_2(\text{UO}_2)_2(\text{MOB})_2(\text{py})_6$ Complexes^a

metal	formula	% C	% H	% N	% U	% M
Co(II)	$\text{C}_{78}\text{H}_{82}\text{N}_6\text{O}_{16}\text{U}_2\text{Co}_2$	47.61 (47.95)	4.09 (4.24)	4.05 (4.30)	24.85 (24.37)	6.02 (6.03)
Ni(II)	$\text{C}_{78}\text{H}_{82}\text{N}_6\text{O}_{16}\text{U}_2\text{Ni}_2$	46.48 (47.95)	4.17 (4.25)	4.62 (4.30)	23.03 (24.37)	5.84 (6.02)
Cu(II)	$\text{C}_{78}\text{H}_{82}\text{N}_6\text{O}_{16}\text{U}_2\text{Cu}_2$	47.83 (47.73)	4.23 (4.22)	4.31 (4.28)	24.23 (24.25)	6.67 (6.48)
Zn(II)	$\text{C}_{78}\text{H}_{82}\text{N}_6\text{O}_{16}\text{U}_2\text{Zn}_2$	46.56 (47.64)	4.18 (4.21)	3.95 (4.27)	24.69 (24.21)	6.82 (6.65)

^a Calculated values appear in parentheses.

was added, and the resulting solution was stirred at room temperature overnight. The volume of solvent was reduced to 100 mL, and a brown solid with a metallic luster was filtered off. Recrystallization from pyridine gave red metallic microcrystals. Elemental analysis for the various complexes are given in Table I.

III. Electrochemistry. The electrochemical setup used for cyclic voltammetry (CV), chronoamperometry (CA), and controlled-potential electrolysis (CPE) has been described in a previous paper.⁴ All electrochemical experiments reported were conducted in pyridine or DMSO with tetraethylammonium perchlorate (TEAP) as the supporting electrolyte. CV and CA experiments were performed by using a hanging-mercury-drop electrode (HMDE). CPE was done with a Hg-pool electrode.

IV. Spectral Characterization. Infrared spectra were recorded with a Nicolet 20DX FTIR spectrometer using KBr pellets. The spectra of all $\text{M}_2(\text{UO}_2)_2(\text{MOB})_2(\text{py})_6$ complexes are very similar. The principal absorptions in the C=O, C=C region and the O—U—O bands are as follows:

	M = Co	M = Ni	M = Cu	M = Zn
$\nu(\text{C}=\text{O}, \text{C}=\text{C}),$ cm^{-1}	1574 1490	1574 1490	1574 1476	1574 1497
$\nu(\text{O}-\text{U}-\text{O}),$ cm^{-1}	906 800	906 800	900 800	906 800

UV-visible spectra were recorded in pyridine with a Perkin-Elmer Lambda 3 spectrophotometer. The protonated ligand exhibits a very strong band centered at 355 nm. The most prominent feature of the $\text{M}_2(\text{UO}_2)_2(\text{MOB})_2(\text{py})_6$ spectra is an intense, symmetric band at about 400 nm with an extinction coefficient of about $10^5 \text{ L}/(\text{mol cm})$. There is also a band at about 285 nm with extinction coefficients of about $3 \times 10^4 \text{ L}/(\text{mol cm})$. The broad intense band at 400 nm obscures any d-d bands.

The fast atom bombardment mass spectrum of a representative complex, $\text{Zn}_2(\text{UO}_2)_2(\text{MOB})_2(\text{py})_6$, in nitrobenzene yielded an intense high mass peak at 1492 mass units. This corresponds to the complex minus all pyridines plus two mass units, i.e. $\text{Zn}_2(\text{UO}_2)_2(\text{MOB})_2 + 2\text{H}$. The intensity of this fragment is 60% of the most intense peak at m/z 270 due to UO_2 .

Results

A complex containing electrochemically inactive Zn^{2+} , $\text{Zn}_4(\text{MOB})_2(\text{py})_4$, was prepared in order to determine whether the complexed ligand is electroactive in the potential range of interest in the $\text{M}_2(\text{UO}_2)_2(\text{MOB})_2(\text{py})_6$ complexes. The CV of $\text{Zn}_4(\text{MOB})_2$ in pyridine shows no electrochemistry in the range of 0.0 to -1.9 V vs SSCE. Thus, in the potential range of interest there is no ligand reduction. Therefore, any reduction processes for the series $\text{M}_2(\text{UO}_2)_2(\text{MOB})_2(\text{py})_6$ are due to M^{2+} and/or UO_2^{2+} .

The electrochemical properties of the binuclear UO_2^{2+} 1,3,7,9-tetraketone, $(\text{UO}_2)_2(\text{DPB})_2(\text{py})_2$, were investigated to study the UO_2^{2+} redox without the complications of the other metal ion, M^{2+} . The CV of $(\text{UO}_2)_2(\text{DPB})_2(\text{py})_2$ in pyridine in the 0 to -1.6 V range consists of one quasi-reversible wave with $E_{1/2} \cong -1.17 \text{ V}$ vs SSCE. At scan rates faster than about 1.00 V/s, the process appears fairly reversible on the basis of i_{pa}/i_{pc} ratios and $i_{pc} \sqrt{v}$ values, 1.00 (± 0.1) and 12.2 (± 0.1), respectively, for a 0.1 mM solution in pyridine with 0.1 M TEAP. Both the peak separations, ΔE_p , and the cathodic peak half-width, $E_{pc} - E_{pc/2}$, are large under these conditions; $\Delta E_p = 225 (\pm 15) \text{ mV}$ and $E_{pa} - E_{pc/2} = 210 (\pm 10) \text{ mV}$.

Chronoamperometry (CA) of $(\text{UO}_2)_2(\text{DPB})_2(\text{py})_2$ was carried out by pulsing the potential from the foot of the reduction wave to -1.40 V . The current decay as a function of time plotted as i_a vs $1/\sqrt{t}$, yielded a straight line of slope $4.87 \mu\text{A}/\sqrt{\text{s}}$ for a 1.00

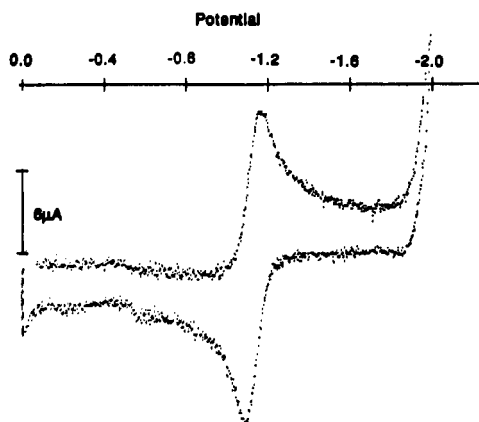
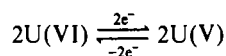


Figure 3. Cyclic voltammogram of 1.00 mM $\text{Co}_2(\text{UO}_2)_2(\text{MOB})_2$ in pyridine at a HMDE. The scan rate is 500 mV/s.

mM solution. Inasmuch as the slope of the straight line is proportional to the number of electrons transferred, n ,⁶ and CPE showed two electrons transferred, the measured slope is taken as indicative of a two-electron process.

The cyclic voltammogram of $\text{Zn}_2(\text{UO}_2)_2(\text{MOB})_2(\text{py})_6$ in the 0 to -2 V range consists of one well-formed CV wave with a cathodic peak potential E_{pc} , at -1.10 V vs SSCE. The characteristics of this wave in the scan rate range 10 mV/s to 20.00 V/s are $E_{1/2} = -1.06$ V, $\Delta E_p = 70 (\pm 5)$ mV, $E_{pc} - E_{pc/2} = 60 (\pm 4)$ mV, and $i_{pa}/i_{pc} = 1.00 (\pm 0.10)$, and $i_{pc} \sqrt{v}$ is constant. On the basis of i_{pa}/i_{pc} and $i_{pc} \sqrt{v}$ values, the electron-transfer process is very nearly reversible.

CA results obtained by pulsing the potential to -1.25 V gave a straight line for i_d vs $1/\sqrt{v}$ of slope $4.67 \mu\text{A}/\sqrt{v}$ for a 1.00 mM solution of $\text{Zn}_2(\text{UO}_2)_2(\text{MOB})_2(\text{py})_6$ in pyridine. CPE showed that two electrons were transferred at -1.25 V. Thus, the CA i_d vs $1/\sqrt{v}$ slope of $4.67 \mu\text{A}/\sqrt{v}$ is consistent with a two-electron transfer due to



occurring at $E_{1/2} = -1.06$ V.

The cyclic voltammogram of $\text{Co}_2(\text{UO}_2)_2(\text{MOB})_2$ in pyridine in the 0 to -2.0 V range exhibits one nearly reversible wave with E_{pc} at -1.16 V vs SSCE. The cyclic voltammogram is shown in Figure 3. The characteristics of the wave at scan rates from 10.0 mV/s to 1.0 V/s are $E_{1/2} = -1.12$ V, $\Delta E_p = 85 (\pm 5)$ mV, $E_{pc} - E_{pc/2} = 73 (\pm 3)$ mV, and $i_{pa}/i_{pc} = 1.00 (\pm 0.05)$, and $i_{pc} \sqrt{v}$ is virtually constant. These data show that the process is quite reversible up to a scan rate of 1.00 V/s. CPE carried out at -1.50 V resulted in the transfer of two electrons. CA results for a 1.00 mM solution of $\text{Co}_2(\text{UO}_2)_2(\text{MOB})_2$ in pyridine yield a straight line plot of i_d vs $1/\sqrt{v}$ with a slope of $4.13 \mu\text{A}/\sqrt{v}$.

The cyclic voltammogram of $\text{Ni}_2(\text{UO}_2)_2(\text{MOB})_2$ in pyridine contains one nearly reversible wave with E_{pc} at -1.18 V. The wave characteristics in the scan range 10 mV/s to 20.00 V/s are $E_{1/2} = -1.14$ V, $\Delta E_p = 70 (\pm 4)$ mV, $E_{pc} - E_{pc/2} = 68 (\pm 4)$ mV, and $i_{pa}/i_{pc} = 1.10 (\pm 0.10)$, and $i_{pc} \sqrt{v}$ is virtually constant. On the basis of the usual experimental parameters, the electron transfer is quite reversible. CPE carried out at -1.50 V results in the addition of two electrons. CA conducted on 1 mM solutions of $\text{Ni}_2(\text{UO}_2)_2(\text{MOB})_2$ in a manner similar to the previous experiments described gave a slope of $4.21 \mu\text{A}/\sqrt{v}$ for the straight line plot of i_d vs $1/\sqrt{v}$.

In DMSO the potential range can be extended sufficiently to observe the CV wave for $\text{Ni(II)} \leftrightarrow \text{Ni(I)}$ in $\text{Ni}_2(\text{UO}_2)_2(\text{MOB})_2$. The solubility in DMSO is quite low, however, so that 5% pyridine must be added to prepare a 1 mM solution. The CV wave due to $\text{U(VI)} \leftrightarrow \text{U(V)}$ at -1.2 V is very little changed from the wave observed in pyridine. The CV wave due to $\text{Ni(II)} \leftrightarrow \text{Ni(I)}$ has

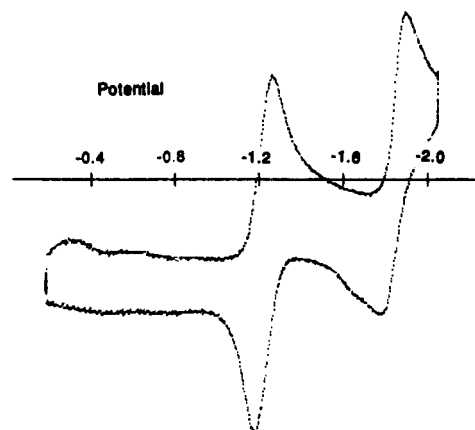


Figure 4. Cyclic voltammogram of $\text{Ni}_2(\text{UO}_2)_2(\text{MOB})_2$ in 95% DMSO-5% pyridine at a HMDE. The scan rate is 500 mV/s.

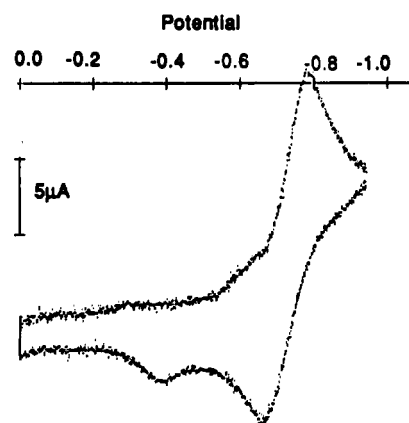


Figure 5. Cyclic voltammogram of 0.50 mM $\text{Cu}_2(\text{UO}_2)_2(\text{MOB})_2$ in pyridine at a HMDE. The scan rate is 100 mV/s.

E_{pc} at about -1.82 V and is quasi-reversible in the scan rate range 10 mV/s to 5.00 V/s. In this scan range ΔE_p increases from 64 to 130 mV, $E_{pc} - E_{pc/2}$ increases from 44 to 67 mV, and i_{pa}/i_{pc} decreases from 0.95 to 0.75. The cyclic voltammogram is shown in Figure 4.

The cyclic voltammogram of $\text{Cu}_2(\text{UO}_2)_2(\text{MOB})_2$ in pyridine exhibits a quasi-reversible wave with E_{pc} at -0.82 V (Figure 5). The peak separation (ΔE_p) and cathodic peak half-width ($E_{pc} - E_{pc/2}$) are relatively constant throughout the scan rate range 100 mV/s to 100.00 V/s. In this range $\Delta E_p = 125 (\pm 25)$ mV and $E_{pc} - E_{pc/2} = 60 (\pm 15)$ mV. The prewave that begins at about -0.5 V makes the values of i_{pa}/i_{pc} suspect. CPE carried out at -1.12 V indicates that four electrons per molecule are transferred. In CA, the slope of the straight line i_d vs $1/\sqrt{v}$ for a 1 mM solution is $8.70 \mu\text{A}/\sqrt{v}$. No CV wave due to $\text{U(VI)} \leftrightarrow \text{U(V)}$ usually observed at -1.2 V for this series is found.

Discussion

Formation of the mixed $\text{UO}_2^{2+}/\text{M}^{2+}$ complexes of the hexaketone, H_2MOB , is synthetically straightforward. Clearly, the ability of the UO_2^{2+} ions to assemble the $[\text{H}_2\text{MOB}]^{2-}$ ligands is as great as it is for the 1,3,5-triketones (Figure 1)³ and the 1,3,5,7-tetraketones (Figure 2).⁴ The same requirement for a fifth axial ligand that yields the cis configuration in uranyl triketonates and forces the uranyl ions to bind to the terminal sites in the 1,3,5,7-tetraketones, results in site-specific UO_2^{2+} binding in the hexaketone. As a result, the ligands are assembled in a manner that facilitates M^{2+} binding at the "inner" coordination positions. This arrangement for the $\text{UO}_2^{2+}/\text{M}^{2+}$ series is shown in Figure 6. Obviously, it is strongly related to the heterobinuclear 1,3,5-triketones and to the heterotrinuclear 1,3,5,7-tetraketones. Although it has not been possible to grow single crystals of any of the $\text{M}_2(\text{UO}_2)_2(\text{MOB})_2(\text{py})_6$ series as yet, there is significant indirect indication that the structures are discrete molecules, as shown in Figure 6, and not high molecular weight

(6) Bard, A. J.; Faulkner, L. R. *Electrochemical Methods*; Wiley: New York, 1980.

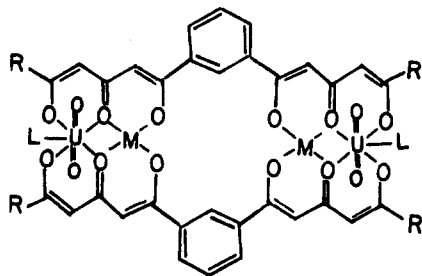
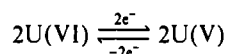


Figure 6. Representation of the $M_2(UO_2)_2(MOB)_2(py)_6$ series. The axial ligands on M have been omitted for clarity.

oligomeric structures resulting from a staggered ligand arrangement. First, the coordinately simpler Cu(II) complex of this ligand easily forms the discrete molecule $Cu_4(MOB)_2(py)_4$, the structure of which is reported in part 1.⁵ The coordination requirements for UO_2^{2+} makes this arrangement very likely in the $M_2(UO_2)_2(MOB)_2(py)_6$ series. Second, the solubility characteristics of the series argue very strongly against high molecular weight oligomers. Third, the analytical results are not consistent with oligomeric products unless the molecular weights were very high. Fourth, the mass spectrum contains the basic molecular unit fragment, $M_2(UO_2)_2(MOB)$, which is consistent with the arrangement shown in Figure 6. By analogy to the structures of $Cu_4(MOB)_2$ ⁵ and $M(UO_2)_2(DBAA)_2(py)_4$,⁴ the M^{2+} ions are about 7.0 Å apart, the two uranium atoms are approximately 14 Å apart, and the U–M distance is about 3.5 Å. Since the uranium atoms are bound to axial oxygens and the M atoms undoubtedly have axially bound pyridines, it is likely that the MOB^{4-} ligands and the four metal ions form a reasonably coplanar arrangement.

The electrochemical behavior of $Zn_4(MOB)_2$, $(UO_2)_2(DPB)_2$, and $Zn_2(UO_2)_2(MOB)_2$ clearly establishes that there are no ligand-based redox processes in the 0 to –1.6 V region and that the redox observed at about –1.1 V is due to $U(VI) \rightarrow U(V)$ reduction. The cyclic voltammogram is indicative of a nearly reversible electron transfer centered at –1.1 V. Both CPE and CA results confirm that the CV waves observed at –1.1 V for $(UO_2)_2(DPB)_2$ and $Zn_2(UO_2)_2(MOB)_2$ are due to the transfer of two electrons. Thus, the process observed is best represented by



For the series $M_2(UO_2)_2(MOB)_2(py)_6$, where $M = Co^{2+}$, Ni^{2+} , and Zn^{2+} , the CV results are very similar. All three exhibit quite reversible two-electron waves. There are however, some interesting differences in the peak separations, ΔE_p , and in the cathodic peak half-width, $E_{pc} - E_{pc/2}$. These parameters in multielectron processes are sensitive to the potential differences for the electron transfers.^{7,8} As the separation between E_1 and E_2 ($\Delta E_{1/2}$) becomes greater, the wave broadens and the peak separation increases. The experimental values of ΔE_p and $E_{pc} - E_{pc/2}$ can be used to calculate $\Delta E_{1/2}$ and, indeed, to simulate the multielectron CV wave.⁹ The average values of ΔE_p and $E_{pc} - E_{pc/2}$ for the series are as follows:

compd	ΔE_p , mV	$E_{pc} - E_{pc/2}$, mV	$\Delta E_{1/2}$, mV
$Co_2(UO_2)_2(MOB)_2(py)_6$	85	73	60
$Ni_2(UO_2)_2(MOB)_2(py)_6$	72	67	50
$Zn_2(UO_2)_2(MOB)_2(py)_6$	70	62	45

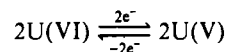
These values have been used to calculate the potential difference between the first-electron and the second-electron transfers, $\Delta E_{1/2}$. It is interesting to contrast these values of $\Delta E_{1/2}$ with those of $M(UO_2)_2(DBAA)_2(py)_4$, where $M = Co^{2+}$, Ni^{2+} , and Zn^{2+} . For the 1,3,5,7-tetraketones in which the M^{2+} ion supplies a four-bond link between uranium atoms, the value of $\Delta E_{1/2}$ are 198, 220, and 256 mV, respectively.⁴ The fact that $\Delta E_{1/2}$ is 3–5 times

as large in $M(UO_2)_2(DBAA)_2(py)_4$ as in $M_2(UO_2)_2(MOB)_2(py)_6$ is the result of a significantly stronger interaction between uranians in the trinuclear tetraketone than in the tetranuclear hexaketone. This is not surprising since the U–U distances are approximately 7 and 14 Å, respectively. It may be that the bridging M^{2+} in $M(UO_2)_2(DBAA)_2$ is more important than the U–U distance, however, since it directly connects the electroactive centers. The importance of M^{2+} in the U–U interaction is supported by the curious periodic increase in $\Delta E_{1/2}$ in the series $M = Fe^{2+}$, Co^{2+} , Ni^{2+} , Cu^{2+} , and Zn^{2+} .

If the two uranium atoms in $M_2(UO_2)_2(MOB)_2$ were totally noninteracting, one would expect a separation $\Delta E_{1/2}$ of 36 mV,^{10,11} arising from purely statistical considerations. This results in a CV wave with $\Delta E_p = 59$ mV and $E_{pc} - E_{pc/2} = 56$ mV. Each of the three compounds, $M = Co^{2+}$, Ni^{2+} , and Zn^{2+} , has a $\Delta E_{1/2}$ value greater than 36 mV, which is indicative of some interaction between the centers. Normally, one would question whether the values observed are sufficiently greater than 36 mV to warrant comment. However, these electron-transfer processes are highly reversible and, therefore, the parameters derived from the CV waves in a reversible scan rate range should be quite dependable. While perhaps not too much should be made of $\Delta E_{1/2}$ values of 45–60 mV versus 36 mV for the noninteracting case, the differences do appear to be experimentally significant. Thus, it is likely that there is a weak but discernible interaction between the redox active centers.

The cyclic voltammogram of $Ni_2(UO_2)_2(MOB)_2$ in DMSO–5% pyridine is of interest since a well-formed wave due to $Ni(II) \leftrightarrow Ni(I)$ is observed under these conditions (Figure 4). Inspection of the data proves that the two-electron $2U(VI) \leftrightarrow 2U(V)$ process is reversible throughout the scan rate range 0.02–20.00 V/s. The average values of ΔE_p (81 mV) and $E_{pc} - E_{pc/2}$ (72 mV) are only slightly greater in DMSO than pyridine. The value of $\Delta E_{1/2}$ for the two UO_2^{2+} electron transfers calculated from these CV parameters is 55 mV. Although the $Ni(II) \leftrightarrow Ni(I)$ electron transfer is only quasi-reversible, it is obvious from the cathodic peak current, i_{pc} , that this is also indicative of a two-electron transfer process. The cathodic peak half-width, which is well under 59 mV, is also indicative of a two-electron transfer process. The narrowness of the cathodic wave indicates that the $E_{1/2}$ values for the sequential transfer of the two electrons are very similar. It is interesting to note that the potential of the nickel wave (–1.81 V) is quite negative in comparison to the potentials of related systems.^{4,12} Typically, the potential for ketonate-type environments is about –1.6 V and for keto iminate environments is about –2.1 V.¹² It is possible that the charge resulting from the reduction of two $U(VI)$ to $U(V)$ centers causes the subsequent $Ni(II) \leftrightarrow Ni(I)$ reductions to shift to a more negative potential. Interestingly, this potential is 200 mV more negative than that of $Ni(II) \rightarrow Ni(I)$ in $Ni(UO_2)_2(DBAA)_2$.⁴

The most unusual electrochemistry in the series is observed for $Cu_2(UO_2)_2(MOB)_2$. Surprisingly, only one CV wave appears in the 0 to –1.2 V potential range. This wave (Figure 5) is quasi-reversible with E_{pc} at –0.82 V and a peak separation, ΔE_p , of 125 mV. The potential is certainly reasonable for $Cu(II) \rightarrow Cu(I)$ reduction in this environment and seems much too positive to be due to $UO_2^{2+} \rightarrow UO_2^+$ reduction. The absence of the usual CV wave at about –1.1 V, which is so characteristic of the $M(UO_2)_2(DBAA)_2$ and $M_2(UO_2)_2(MOB)_2$ complexes, is unexpected. CA results plotted as i_d vs $1/\sqrt{v}$ yielded a slope of 8.70 $\mu A/\sqrt{s}$. This value is almost exactly twice the value obtained for the two-electron



process observed in the other complexes where $M = Zn$, Ni , and Co . Thus, on the basis of CA, the CV wave at –0.8 V is due to

(7) Polycn, D. S.; Shain, I. *Anal. Chem.* **1966**, *38*, 370.

(8) Meyers, R. L.; Shain, I. *Anal. Chem.* **1969**, *41*, 980.

(9) For example: Sokol, W. F.; Evans, D. H.; Niki, K.; Yagi, T. *J. Electroanal. Chem. Interfacial Electrochem.* **1980**, *108*, 108.

(10) Falanigan, J. B.; Margel, S.; Bard, A. J.; Anson, F. C. *J. Am. Chem. Soc.* **1978**, *100*, 4248.

(11) Ammas, F.; Saviant, J. M. *J. Electroanal. Chem. Interfacial Electrochem.* **1973**, *47*, 115, 215.

(12) Lintvedt, R. L.; Ranger, G.; Kramer, L. S. *Inorg. Chem.* **1986**, *25*, 2635.

the transfer of four electrons. CPE results confirm that four electrons per molecule are transferred at -1.1 V. There would appear to be only two possibilities for a four-electron process: (1) all four electrons are used to reduce Cu(II) to Cu(0) and no UO_2^{2+} electrochemistry is observed or (2) all four metal ions are reduced, yielding two Cu(I) and two U(V) centers. The quasi-reversibility of the CV wave argues strongly against the production of Cu(0) since formation of Cu(Hg) amalgam would preclude any significant degree of reversibility. Thus, one must conclude that the four electrons transferred ultimately reside on the four metals. Why the U(VI) \rightarrow U(V) reduction potential should be shifted by $+300$ mV in $\text{Cu}_2(\text{UO}_2)_2(\text{MOB})_2$ is not at all clear. Nor is it obvious why the reduction potentials of Cu(II) and UO_2^{2+} should be so similar in this compound. The unique feature of $\text{Cu}_2(\text{UO}_2)_2(\text{MOB})_2$ compared to the others in the series is that the transition-metal ion (Cu^{2+}) reduces more positively than the UO_2^{2+}

ions. It is possible that the formation of Cu^+ centers at -0.8 V produces geometric and electronic changes that facilitate the reduction of UO_2^{2+} and/or stabilize UO_2^+ .

The compound $\text{Cu}_2(\text{UO}_2)_2(\text{MOB})_2$ is of considerable interest since the observation of well-behaved four-electron-transfer electrochemistry is very rare. The tetranuclear Cu complex of MOB^{4-} also exhibits four-electron-transfer electrochemistry at essentially the same potential.⁵ The CA and CPE results for the two compounds are very similar and consistent with the transfer of four electrons. However, the CV results for $\text{Cu}_2(\text{UO}_2)_2(\text{MOB})_2$ show that the electron transfer is significantly more reversible in this molecule than in $\text{Cu}_4(\text{MOB})_2$.

Acknowledgment. We are grateful to the National Science Foundation (Grant CHE86-10808) for financial support of this research.

Contribution from the Institut für Anorganische Chemie der Universität Hamburg, D-2000 Hamburg 13, FRG

Oxovanadium Alkoxides: Structure, Reactivity, and ^{51}V NMR Characteristics. Crystal and Molecular Structures of $\text{VO}(\text{OCH}_2\text{CH}_2\text{Cl})_3$ and $\text{VOCl}_2(\text{THF})_2\text{H}_2\text{O}$

Wolfgang Priebsch and Dieter Rehder*

Received December 14, 1989

The vanadyl esters $\text{VO}(\text{OR})_3$ ($\text{R} = \text{Me, Et, Pr, iPr, sBu, tBu, CH}_2\text{CH}_2\text{F, CH}_2\text{CH}_2\text{Cl, CH}_2\text{CCl}_3$) have been prepared and their association properties in pentane investigated by ^{51}V NMR. Limiting (low concentration) $\delta(^{51}\text{V})$ values depend on the bulk of R (highest ^{51}V shielding for tBu). Shielding decreases with increasing concentration (more pronounced for small R groups), owing to the formation of oligomers, probably connected by μ -OR groups. The X-ray diffraction study of $\text{VO}(\text{OCH}_2\text{CH}_2\text{Cl})_3$ (space group $P\bar{1}$; $a = 766.2$ (2) pm, $b = 907.5$ (4) pm, $c = 957.0$ (2) pm, $\alpha = 82.08$ (3) $^\circ$, $\beta = 66.90$ (2) $^\circ$, $\gamma = 79.42$ (3) $^\circ$) reveals dimer association of molecules belonging to adjacent unit cells via long V-OR bonds (226.1 (2) pm), and a trigonal-bipyramidal geometry for each monomeric unit. From the reaction between VOCl_3 and diols (glycol, 1,3-propanediol, 1,2-, 2,3-, 1,3-, and 1,4-butanediol), complexes are obtained that contain the $\{\text{VOCl}(\text{OR})_2\}$ and $\{\text{VOCl}_2\text{OR}\}$ moieties and the alcohol coordinated in the monofunctional or bifunctional (chelating and bridging) mode. The ^{51}V NMR spectrum of $\text{VOCl}_2\text{OCH}(\text{Me})\text{CH}(\text{Me})\text{OH}$ exhibits resolved ^{51}V - $^{35,37}\text{Cl}$ coupling: $J(^{51}\text{V}-^{35}\text{Cl}) = 100$ Hz; $J(^{51}\text{V}-^{37}\text{Cl}) = 83$ Hz. $\text{V}^{\text{VOCl}_2(\text{OCH}_2\text{CH}_2\text{CH}_2\text{CH}_2\text{OH})}$ reacts with 1,4-butanediol to form $\text{V}^{\text{VOCl}_2(\text{THF})_2(\text{OH})_2}$ (space group $C2/c$; $a = 1221.7$ (5) pm, $b = 1710.9$ (7) pm, $c = 922.3$ (4) pm, $\beta = 138.53$ (22) $^\circ$). In the presence of VOCl_3 , THF undergoes ether splitting, chlorination, and coordination to vanadium to yield $\text{VOCl}_2(\text{OCH}_2\text{CH}_2\text{CH}_2\text{Cl})$.

Introduction

Metal alkoxides are valuable precursors for electronic and ceramic materials,¹ and volatile species, such as the alkoxides of V^{IV} and V^{V} , are potential candidates for chemical vapor deposition of metal and metal oxides. A more classical and nonetheless rapidly developing field of application for vanadium alkoxides and related compounds (e.g. complexes with ketols) is their use as catalysts in polymerization² and oxidation reactions.³ Furthermore, interest has recently focused on vanadyl alkoxides $\text{VO}(\text{OR})_{3-n}(\text{OH})_n$ (esters of the hypothetical orthovanadic acid) as model compounds for the interaction of vanadate with the tyrosine and serine constituents of enzymes involved in phosphorylation reactions, which are commonly inhibited or stimulated by vanadate.⁴ A V-OR bond has also been proposed for the coordination

environment of V^{V} in vanadate-dependent haloperoxidase from a marine brown alga on the basis of an EXAFS study, which revealed one rather short V-O single bond.^{4f}

In aqueous media, OH-functional molecules such as monoalcohols,^{5a,b} diols,^{5c,d} saccharides,^{5d} nucleosides,^{5e,6a} lactic acid,^{5f}

- (1) Bradley, D. C. *Chem. Rev.* **1989**, *89*, 1317.
- (2) (a) Jiao, S.; Su, D.; Yu, D.; Hu, L. *Chin. J. Polym. Sci.* **1988**, *6*, 135. (b) Tsuchida, E.; Yamamoto, K.; Jikei, M.; Nishide, H. *Macromolecules* **1989**, *22*, 4313. (c) Aliwi, S. M.; *J. Photochem. Photobiol. A* **1988**, *44*, 179.
- (3) (a) Barret, R.; Pautet, F.; Daudon, M.; Sabot, J. F. *Pharm. Acta Helv.* **1987**, *62*, 348. (b) Samarik, V. Ya.; Pikh, Z. G. *Khim. Tekhnol. (Kiev)* **1987**, *22*. (c) Moiseeva, N. I.; Gekhman, A. E.; Blyumberg, E. A.; Moiseev, I. I. *Kinet. Katal.* **1988**, *29*, 970. (d) Baevskii, M. Yu.; Litvintsev, I. Yu.; Sapunov, V. N. *Kinet. Katal.* **1988**, *29*, 575. (e) Martinez de la Cuesta, P. J.; Ruz Martinez, E.; Aguiar Garcia, J. *Grasas Aceites (Seville)* **1989**, *39*, 82.

- (4) Selected examples are the inhibition of (a) alkaline phosphatase (Crans, D. C.; Bunch, R. L.; Theisen, L. A. *J. Am. Chem. Soc.* **1989**, *111*, 7597), (b) Na,K-ATPase (Cantley, L. C., Jr.; Cantley, L. G.; Josephson, L. J. *Biol. Chem.* **1978**, *253*, 7361) and (c) ribonucleases (Kostrewa, D.; Choe, Hui-Woog.; Heinemann, U.; Saenger, W. *Biochemistry* **1989**, *28*, 7592. Borah, B.; Chen, Chi-wan.; Egan, W.; Miller, M.; Wlodawer, A.; Cohen, J. S. *Biochemistry* **1985**, *24*, 2058), and the stimulation of (d) serine sulfhydrylase (Meisch, H.-U.; Kappesser, S. *Biochim. Biophys. Acta* **1987**, *925*, 234) and (e) the diphosphoglycerate phosphatase activity of phosphoglycerate mutase (Carreras, J.; Climent, F.; Bartrons, R.; Pons, G. *Biochim. Biophys. Acta* **1982**, *705*, 238). (f) Arber, J. M.; de Boer, E.; Garner, C. D.; Hasnain, S. S.; Wever, R. *Biochemistry* **1989**, *28*, 7968.
- (5) (a) Tracey, A. S.; Gresser, M. J. *Can. J. Chem.* **1988**, *66*, 2570. (b) Tracey, A. S.; Gresser, M. J. *Proc. Natl. Acad. Sci. U.S.A.* **1986**, *83*, 609. (c) Gresser, M. J.; Tracey, A. S. *J. Am. Chem. Soc.* **1986**, *108*, 1935. (d) Tracey, A. S.; Gresser, M. J. *Inorg. Chem.* **1988**, *27*, 2695. (e) Tracey, A. S.; Gresser, M. J.; Liu, S. J. *Am. Chem. Soc.* **1988**, *110*, 5869. (f) Tracey, A. S.; Gresser, M. J.; Parkinson, K. M. *Inorg. Chem.* **1987**, *26*, 629.
- (6) (a) Geraldies, C. F. G. C.; Castro, M. M. C. A. *J. Inorg. Biochem.* **1989**, *35*, 79. (b) Caldeira, M. M.; Ramos, L.; Cavaleiro, A. M.; Gil, V. M. S. *J. Mol. Struct.* **1988**, *174*, 461. (c) Ehde, P. M.; Andersson, I.; Pettersson, L. *Acta Chem. Scand.* **1989**, *43*, 136.